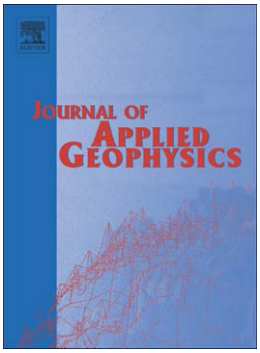

Optimizing the number of stations in arrays measurements: Experimental outcomes for different array geometries and the f-k method

S. Rosa-Cintas, J.J. Galiana-Merino, P. Alfaro, J. Rosa-Herranz

PII: S0926-9851(13)00285-1
DOI: doi: 10.1016/j.jappgeo.2013.12.008
Reference: APPGEO 2397

To appear in: *Journal of Applied Geophysics*

Received date: 13 January 2013
Accepted date: 10 December 2013

Please cite this article as: Rosa-Cintas, S., Galiana-Merino, J.J., Alfaro, P., Rosa-Herranz, J., Optimizing the number of stations in arrays measurements: Experimental outcomes for different array geometries and the f-k method, *Journal of Applied Geophysics* (2013), doi: 10.1016/j.jappgeo.2013.12.008

OPTIMIZING THE NUMBER OF STATIONS IN ARRAYS MEASUREMENTS: EXPERIMENTAL OUTCOMES FOR DIFFERENT ARRAY GEOMETRIES AND THE F-K METHOD

S. Rosa-Cintas[1*], J.J. Galiana-Merino[2,3], P. Alfaro[1], J. Rosa-Herranz[2,3]

[1]Dpto. Science of Earth and Environmental Science, University of Alicante, P.O. Box 99, E-03080 Alicante, Spain.

[2]Dpto. Physics, Systems Engineering and Signal Theory, University of Alicante, P.O. Box 99, E-03080 Alicante, Spain.

[3]University Institute of Physics Applied to Sciences and Technologies, University of Alicante, P.O. Box 99, E-03080 Alicante, Spain.

(*) Corresponding author: sergio.rosacintas@ua.es

Email addresses:

JJGM: juanjo@dfists.ua.es

PA: pedro.alfaro@ua.es

JRH: julio.rosaherranz@ua.es

OPTIMIZING THE NUMBER OF STATIONS IN ARRAY MEASUREMENTS: EXPERIMENTAL OUTCOMES FOR DIFFERENT ARRAY GEOMETRIES AND THE F-K METHOD

S. Rosa-Cintas[1*], J.J. Galiana-Merino[2,3], P. Alfaro[1], J. Rosa-Herranz[2,3]

[1]Dpto. Science of Earth and Environmental Science, University of Alicante, P.O. Box 99, E-03080 Alicante, Spain.

[2]Dpto. Physics, Systems Engineering and Signal Theory, University of Alicante, P.O. Box 99, E-03080 Alicante, Spain.

[3]University Institute of Physics Applied to Sciences and Technologies, University of Alicante, P.O. Box 99, E-03080 Alicante, Spain.

(*) Corresponding author: sergio.rosacintas@ua.es

ABSTRACT

Array measurements have become a valuable tool for site response characterization in a non-invasive way. The array design, i.e. size, geometry and number of stations, has a great influence in the quality of the obtained results. From the previous parameters, the number of available stations uses to be the main limitation for the field experiments, because of the economical and logistical constraints that it involves.

Sometimes, from the initially planned array layout, carefully designed before the fieldwork campaign, one or more stations do not work properly, modifying the prearranged geometry. Whereas other times, there is not possible to set up the desired array layout, because of the lack of stations. Therefore, for a planned array layout, the

number of operative stations and their arrangement in the array become a crucial point in the acquisition stage and subsequently in the dispersion curve estimation.

In this paper we carry out an experimental work to analyze which is the minimum number of stations that would provide reliable dispersion curves for three prearranged array configurations (triangular, circular with central station and polygonal geometries). For the optimization study, we analyze together the theoretical array responses and the experimental dispersion curves obtained through the f-k method.

In the case of the f-k method, we compare the dispersion curves obtained for the original or prearranged arrays with the ones obtained for the modified arrays, i.e. the dispersion curves obtained when a certain number of stations *n* is removed, each time, from the original layout of *X* geophones. The comparison is evaluated by means of a misfit function, which helps us to determine how constrained are the studied geometries by stations removing and which station or combination of stations affect more to the array capability when they are not available. All this information might be crucial to improve future array designs, determining when it is possible to optimize the number of arranged stations without losing the reliability of the obtained results.

Keywords: *Array design, Array optimization, Seismic noise, f-k technique*

1. INTRODUCTION

Ambient noise based studies constitute an extended procedure for microzonation purposes, specially suitable for zones where conventional seismic methods are difficult or

even prohibitive to implement, such as urban or environmentally sensitive areas (e.g. Bard, 1994; Lebrun et al., 2001; Souriau et al., 2007; D'Amico et al., 2008; Mundepi et al., 2010).

Within the microtremor survey method, array analysis constitutes a valuable tool for site response characterization, obtaining the dispersion curve at the study area and then estimating the Vs profile by means of an inversion procedure (Ohrnberger et al., 2004; Parolai et al., 2007; Endrun et al., 2010). Some of the most used array techniques are the frequency-wavenumber (f-k) (Capon, 1969; Lacoss et al., 1969; Asten and Henstridge, 1984; Horike, 1985; Ohrnberger, 2001), the spatial autocorrelation (SPAC) (Aki, 1957; Roberts and Asten, 2004) and the extended spatial autocorrelation (ESAC) (Ohori et al., 2002; Okada, 2003).

Because of the economical and logistical constraints that limit the number of stations used in the field experiments, the election of an appropriate array size and geometry is a key factor to enhance the resultant dispersion curves (SESAME, 2005).

Circular layout with an odd number of stations is shown in many works as a good way to optimize the array layout for a given number of sensors (Poggi and Fäh, 2010; Endrun et al., 2010; Rosa-Cintas et al., 2011; Mahajan et al., 2011). It presents large aperture, as well as small inter-station distances, which provide good resolution and aliasing capabilities, respectively. Moreover, circular layout displays a good azimuthal sampling, showing homogeneous geometry for all the arrival directions.

Other array shapes reported in literature are triangular (Asten et al., 2004; Chun-Hsiang et al., 2009; Stephenson et al., 2009; Mundepi et al., 2010), seven-station hexagonal (Asten et al., 2000, 2004 and Asten, 2006), semi-circular (Chouet et al., 1998;

Asten et al., 2004), cross-shaped (Ohori et al., 2002; Asten et al., 2004), T-shaped (Parolai et al., 2007; Picozzi et al., 2010), L-shaped (Horike, 1985) and irregular-geometry (Parolai et al., 2006, 2007 and 2010; Picozzi et al., 2009; Endrun et al., 2010; Boxberger et al., 2011).

Traditionally, the performance of a given array layout is evaluated by the theoretical array response pattern (also known as beam pattern), which provides insights about the aliasing effects and the maximum resolution limits, in terms of the maximum and minimum wavenumbers, respectively. However, these results only depend on the array configuration, without taking into account the nature and direction of the noise wavefield, that is the slowness and the wavenumber of the recorded seismic phases. Therefore, it is also important to consider the array technique used and then, the obtained experimental dispersion curve, which provides insights of the effective wavenumber range that can be reached, i.e. the real array capability.

In this way, several papers study the array optimization in terms of geometry and number of stations by using the SPAC method. Asten et al. (2004) and Asten (2006) numerically analyze the expected behavior of the SPAC spectrum with different array configurations and azimuth samplings. They conclude that for triangular arrays the limited spatial averaging provided by the placement of geophones is compensated by greater averaging provided by a larger azimuthal spread of energy sources. For semi-circular arrays, their use provides significant improvements in the SPAC technique when dominant seismic noise sources exist at fixed locations, while the hexagonal array is superior in maximizing the range of detectable wavelengths.

In other researches, Cho et al. (2004, 2006 and 2008) further evaluated the maximum expected errors on SPAC spectra, with respect to frequency and number of sensors, using different wavefield scenarios. Also Okada (2006) completed a similar study, considering the minimum number of stations required by a circular array for efficient data collection in terms of analytical efficacy and field effort. He concludes that the 3-stations circle array, when compared with other 4-, 5-, and 9-station arrays, is the most efficient and favorable for observation of microtremors, if the SPAC coefficients are used up to a frequency at which the coefficient takes the first minimum value. He also establishes that the Nyquist wavenumber is the most influential factor that determines the upper limit of the frequency range up to which the valid SPAC coefficient can be estimated.

More recently, Claprood and Asten (2010) propose a methodology to experimentally assess the reliability of the SPAC method on observations made with a limited number of sensors; investigating parameters such as the number of sensors (pair of sensors, triangular or hexagonal arrays), the length of the time series and the frequency interval, by analyzing the behavior of the real and imaginary components of the observed coherency spectra.

Concerning the array optimization with f-k method, we found less researching in the literature. Barber (1959) and Haubrich (1968) showed ways in which the beam pattern can be understood and optimized for a given number of sensors. Later, Kind et al. (2005) presented an application based on high-resolution beamforming f-k method applied to the vertical component of the measurements. They point out that although the

beamforming method does not depend on the specific array configuration, it does play an important role controlling the wavenumber resolution properties of the array.

In a recent work, Picozzi et al. (2010) propose to correct the f-k power spectral density function (PSDF) estimate for the effects introduced by the array transfer function, in analogy to the correction for the instrumental response of seismological data. This methodology qualitative improves the f-k PSDF estimation, which has been traditionally based on the selection of a particular array configuration by a visual check of the array transfer function characteristics (i.e., Wathelet, 2005).

The SPAC method is usually preferred in the literature to the f-k one, because of its requirement of fewer sensors to achieve the same array resolution and for its better resolution at low frequencies, corresponding to deep materials, for the same array aperture (Asten and Henstridge, 1984; Chávez-García et al., 2005; Okada, 2006; Claprood and Asten, 2010). In this way, Claprood and Asten (2010) propose an alternative method to detect the predominant propagation direction of microtremor wavefield, based on the azimuthal distribution of the mean square of residuals factors for SPAC observations. This new approach is presented as an interesting alternative to the traditional f-k method, which has poor resolution at low frequencies, when using a restricted number of sensors (i.e., 3- or 6-station arrays) (Claprood and Asten, 2010).

As shown in the mentioned papers, array design constitutes an important issue in the microtremor survey method, even more because no an ideal array outline exists, since every configuration has both advantages and disadvantages over other types. For that reason, stations layout should be carefully planned before a fieldwork campaign. Unfortunately, sometimes, one or more stations do not work properly, modifying the

prearranged geometry (e.g. Mundepi et al., 2010; Rosa-Cintas et al., 2011). In other cases, there is not possible to set up the desired array layout because of the lack of stations. Therefore, for a planned array layout, the number of operative stations and their arrangement in the array become a crucial point in the acquisition stage and subsequently in the dispersion curve estimation.

In this paper we have carried out an experimental work to carefully analyze the station missing effect over different prearranged array configurations (triangular, circular with central station and polygonal geometries) and then, determine the minimum number of stations that would provide reliable dispersion curves for the analyzed arrays.

For the optimization study, we analyze together the theoretical array responses and the experimental dispersion curves obtained through the f-k method.

In the case of the f-k method, we compare the dispersion curves obtained for the original or prearranged arrays with the ones obtained for the modified arrays, i.e. the dispersion curves obtained when a certain number of stations n is removed, each time, from the original layout of X geophones. This comparison study will help us to evaluate the possibility of obtaining reliable dispersion curves using $(X\text{-}n)$ stations arrays instead of the original arrays with X stations. All this information will be valuable to improve future array designs, analyzing when it is possible to optimize the number of arranged stations, without losing the reliability of the obtained results.

2. METHODOLOGY

2.1 *Frequency-wavenumber method*

Surface waves are considered the dominant and most coherent component forming part of seismic noise (Toksöz and Lacoss, 1968). When the seismic noise is recorded through an array of vertical seismometers simultaneously, the characteristics of the Rayleigh wave propagation in the medium can be extracted, that is the Rayleigh wave dispersion curve. The array data analysis can be carried out through different techniques, among which the frequency-wavenumber analysis (f-k) (Capon, 1969; Lacoss et al., 1969) is the technique that we have used.

This method is based on the estimate of the frequency-wavenumber spectral density function, which provides the power as a function of the frequency and the vector velocities of the propagating waves. Since the propagation direction and the velocity are usually unknown beforehand, the search is performed on a dense wavenumber grid for each frequency. The maximum beam power on this grid provides an estimate of the propagation direction and the velocity of the plane waves. For that, the stationary assumption in both time and two spatial coordinates has to be fulfilled.

The way of estimating the power spectrum classifies the method in two groups: the beam-forming method (BFM) (Lacoss et al., 1969), and the maximum likelihood method (MLM) (Capon, 1969). The MLM method increases the capability to distinguish between two waves travelling at close wavenumbers, improving the resolving power (Okada, 2003; Parolai et al., 2007; Endrun et al., 2010).

For our study we use the BFM method because it is less sensitive to measurements errors (Capon, 1969) than MLM, although it exhibits lower resolving power. More details about both methods can be found in Horike (1985) and Okada (2003).

2.2 Data acquisition

The seismic noise measurements were recorded around the village of Catral, which is located in the central part of the Bajo Segura Basin (southeast Spain). This area constitutes a well-known place studied in previous works (Rosa-Cintas et al., 2011, 2012a, 2012b).

The Bajo Segura Basin constitutes a Neogene-Quaternary depression developed in the northeast part of the Betic Cordillera (Delgado et al., 2000 and 2003). The basin has an elongated morphology in the ENE-WSW direction and it is controlled principally by two faults, the Crevillente fault to the north and the Bajo Segura fault to the south (Alfaro et al., 2002). The basement of the basin is mainly composed of limestones and marls (Triassic to Cretaceous age), while in the sedimentary fill of the basin we can find sandstones and marls, with levels of conglomerates and presence of gypsums, with ages comprised from the Late Miocene right up to the present time (Soria et al., 1999; Delgado et al., 2000 and 2003).

Though the seismicity in the study area is moderate to low, several episodes of destructive earthquakes have taken place during the last centuries, like the 1829 Torrevieja earthquake, with a maximum intensity EMS-98 of IX-X (Martínez Solares and Mézcua, 2002).

The array was arranged using seismic refraction/reflection equipment consisting of twenty-four 10 Hz vertical geophones connected to a multichannel seismic recorder (RAS-24 Exploration Seismograph). The data acquisition was taken during 30 minutes at a sample rate of 500 Hz.

The same equipment was recently used by Rosa-Cintas et al. (2012b), in a similar way to Galiana-Merino et al. (2011), in order to study the suitability of low-cost geophones for taking array measurements of ambient noise and estimating the dispersion curves through the f-k and the ESAC techniques. The comparison of the results obtained by 1Hz-sensors and 10Hz-vertical-geophones arrays in terms of power spectra density functions and dispersion curves demonstrate the suitability of standard seismic refraction/reflection equipment for ambient noise array measurements.

For the analyzed arrays and methods, the study reveals the capability of the 10 Hz vertical geophones to analyze frequencies much smaller than their natural one, reaching values down to 2 Hz for the large-aperture arrays. However, the effectiveness of the 10 Hz geophones should be tested at each site, as it depends on the level of noise in the studied area. If such level is strong enough at the frequency we want to look at, likely also the 10 Hz geophones are capable to capture a part of the energy even at frequencies well below 10 Hz. Similar works studying the broadening of the usable frequency range for different kinds of sensors can be found in the literature, e.g. Strollo et al. (2008a and b), applied to the H/V technique (Nakamura, 1989).

The studied zone is the same that in Rosa-Cintas et al. (2012b): the Bajo Segura Basin. Thus, based on the assumption of a stochastic wavefield, which is stationary both in time and space (Okada, 2003; Endrun et al., 2010; Rosa-Cintas et al., 2012b), we can consider proved the suitability of the 10 Hz vertical geophones for taking array measurements of ambient noise and estimating the dispersion curves down to frequencies of 2-3 Hz.

3. ARRAY DESIGN

The analyzed array configurations and their associated theoretical array responses are represented in Figure 1: triangular (7-geophones), circular with central station (9-geophones) and polygonal (9-geophones) (Figures 1a, 1b and 1c, respectively). A set of eighteen geophones was precisely arranged using measuring tape in order to create a general array configuration of 25 m of aperture, which comprised all the analyzed geometries. Each one of the studied layouts is then derived from the general one, by removing a certain number of geophones before the data analysis. This way of performing the arrays allows simultaneous registers for all the studied geometries.

The objective is to generate three layouts with similar characteristics in both number of stations and maximum aperture, despite the maximum inter-station distance is of 25 m in the circular and polygonal arrays and of 21.65 m in the triangular array, as it is inscribed in the circular geometry.

In Table 1 we show the wavenumber limits, kmax and kmin/2 values, corresponding to the theoretical response of the arrays represented in Figure 1. kmax parameter provides insights about the aliasing effects and it is related to the lateral peaks of the theoretical array response; whereas the kmin value determines the resolution capability of the array to distinguish waves travelling at close wavenumbers and it is linked to the width of the central peak (Wathelet, 2005).

From the values presented in Table 1, we can establish that the circular geometry is the one that provides a wider wavenumber range for the analysis of the computed dispersion curve. Concerning the maximum resolution limit (kmin/2), the circular shape shows lower limit value than the other two geometries, being almost the half of the

polygonal one. In the case of the triangular shape, it is normal that a higher limit value is provided, because the aperture is smaller and it is a 7-stations array front the other two 9-stations arrays. But the polygonal array, conceived to join the largest aperture of the circular geometry with the shortest inter-station distances presented in the general array, shows unfortunately the highest maximum resolution limit, which actually means the shortest capacity of analysis at low frequencies. It provides even higher limit than the triangular geometry, which presents smaller aperture but providing higher spatial symmetry.

Regarding the aliasing limit (kmax), the analyzed 9-geophones arrays provide considerably better results than the triangular one, with two stations less. The analyzed polygonal geometry, with the shortest inter-station distances, provides the highest limit, which means the biggest capacity of analysis at high frequencies. The difference respect to the circular geometry is small; nevertheless a small variation in the wavenumber domain can have a strong impact at high frequencies.

4. ARRAY OPTIMIZATION STUDY

For the present study, we analyze together the theoretical array responses and the experimental dispersion curves obtained through the f-k method.

The natural way to evaluate the influence of the array geometry and the number of stations is studying the theoretical array response. It is important that the array configuration provides a symmetric theoretical response respecting to the central peak, which ensures an equal response for waves coming from all azimuths. In contrast, the good performance of arrays that provide aligned theoretical responses will depend on the

direction of the incoming waves. The theoretical response also provides insights about the aliasing effects and the maximum resolution limits, in terms of the maximum and minimum wavenumbers, respectively.

However, these results just show the theoretical array response and they only depend on the array configuration. The recorded measurements depend on the array configuration, but also on the nature and direction of the incoming noise wavefield. Thus, for the aim of this paper, we also consider that it is important to study the obtained dispersion curves, which provide insights of the effective wavenumber range that can be reached with a lower number of stations.

For the experimental analysis, we only presuppose the general suppositions considered for array measurements: i.e. homogeneous and isotropic soil conditions under the area covered by the array (Okada, 2003); and stochastic and stationary noise wavefield in both space and time (Okada, 2003; Parolai et al., 2007; Endrun et al., 2010). In Figure 2, we show the directionality of the recorded seismic noise at four different frequencies, selected from the analyzed frequency range. The f-k analysis of the circular configuration has been chosen to display the noise sources distribution, since this layout provides the highest central symmetry of all the analyzed ones. The panels allow a clear identification of the maxima for all the frequencies depicted. The distribution of the noise sources is approximately isotropic with slight highlight of the maxima in directions E-W and NW-SE.

In Figure 3, the dispersion curves estimated with the original geometries are presented. We also show the wavenumber limits functions for kmax/2 and kmin/2 values,

based on Table 1 parameters, to establish the theoretical valid wavenumber interval for each dispersion curve (Wathelet, 2005).

At this point we would like to indicate that geophone #10 did not work properly during the acquisition time, so it was not considered for the data analysis of the circular array. Anyway, we can check that the obtained dispersion curve does not differ from the ones obtained with the triangular and the polygonal arrays, Thus, for the purposes of the present work, we could start establishing that the lack of one station in the 9-station circular array does not affect to the obtained dispersion curve (considering the mean value ± standard deviation in the valid frequency interval).

From Figure 3, it can be noticed that the three obtained dispersion curves are very similar. The differences among the analyzed array configurations can be found in the valid wavenumber range (given by kmin/2 and kmax/2), as it was previously observed in Table 1. The intersection of the obtained dispersion curves with the theoretical wavenumber limits allows establishing the frequency intervals of analysis for the dispersion curves. In the case of the circular array, the obtained dispersion curve does not intersect with the kmax/2 limit, but we can observe that for frequencies from about 15 Hz onward the phase velocity starts to increase, which is indicative of the spatial aliasing. Attending to this criterion, the frequency interval associated to each geometry is shown by different color areas in Figure 3.

For the subsequent study we have decided to set the upper limit of analysis at 10 Hz for the circular and polygonal arrays, as we are more interested in checking the behavior of the dispersion curves at low frequencies. Therefore, the analyzed frequency

ranges are: 4-9.5 Hz in the triangular layout, 3.5-10 Hz in the circular one and 5-10 Hz in the polygonal geometry.

The f-k analysis was carried out using GEOPSY software from the Sesarray package (www.geopsy.org). The recorded signals were divided in data windows of frequency dependent length, including 30 periods of the frequency in focus. The identification of the high power regions in the wavenumber plane was conducted through the selection of two parameters: the grid size (kmax/2), which defines the usable range for the search of the maximum beam power and it is bounded by the aliasing limit; and the grid step (kmin/4), which defines the grid resolution.

For the optimization study, we compare the dispersion curves obtained with the original array layouts with the dispersion curves computed for the modified arrays, i.e. the dispersion curves obtained when a certain number of stations *n* is removed, each time, from the original layout of *X* geophones. For the analysis of the modified arrays, the grid parameters were remained constant, being the same that the ones used with the corresponding original arrays. In this way, we can compare both curves in the same frequency band and then, evaluate the viability of using *(X-n)* geophones, instead of *X* ones, for the estimation of the dispersion curves. In Figure 4, we show the theoretical resolution limits (i.e. the kmin/2 values) of the original and the reduced configurations that provide at least acceptable results. In the case of the reduced configurations, different resolution limit values are obtained for the same number of geophones, depending on their distribution. Thus, a resolution limit range is provided when using *(X-n)* geophones. In general, the resolution limit increases as the number of geophones is reduced,

decreasing the theoretical array capability, although the minimum value can be also reached for some reduced configurations.

We have also analyzed different layouts that can be considered equivalent, as they have the same geometry but different azimuths respecting to the incoming seismic noise. Thus, these equivalent geometries represent rotation of certain angles for the same layout. The aim of analyzing these equivalent geometries is to test the robustness of the modified arrays to anisotropic ambient noise.

In order to show the significance (or not) of the bias, the mean value and the standard deviation of the dispersion curves obtained with the original and the modified array layouts are shown in Figures 5, 7 and 8. These differences have also been quantitatively evaluated through a misfit function, which has been computed in the analyzed frequency intervals by means of the following equation:

$$m = \sqrt{\frac{1}{N}\sum_{i=1}^{N}\left(\frac{x_S(i)-x_G(i)}{\sigma_S(i)}\right)^2}\cdot\sqrt{\frac{1}{N}\sum_{i=1}^{N}\left(\frac{x_S(i)-x_G(i)}{\sigma_G(i)}\right)^2} \quad (1)$$

where x_S and σ_S are the mean value and the standard deviation of the dispersion curve obtained for the original array at the frequency sample i; x_G and σ_G are the mean value and the standard deviation of the dispersion curve obtained for each modified array at the frequency sample i; and N is the number of frequency samples.

The graphical comparison of the dispersion curves and the associated misfit values are shown for all the tested geometries in the annexes chapter. We refer to the annexes by using the nomenclature: 'A.X.N'; where A means Annex, X denotes the array shape (i.e., T, Triangular; C, Circular and P, Polygonal) and N refers to the number of

annexes. In Figures 5, 7 and 8, we represent the cases that show the lowest and the highest misfit values for every array shape and number of geophones tested.

The similarity of the three original dispersion curves helps for the misfit comparison among the different tested geometries, in order to determine which array configuration is less constrained by stations removing.

In Table 2, we group the different analyzed cases according to the obtained misfit values and we compare the three array layouts combinations, for each determined number of geophones. The dispersion curves are classified in three groups according to the misfit values: ($m \leq 0.2$) comprises the curves that can be considered as good ones, ($0.2 < m \leq 0.5$) the curves that can be considered as acceptable and ($0.5 < m$) the unacceptable ones.

In the case of all the circular and polygonal configurations tested with 8 and 7 stations, they provide good dispersion curves, with misfits down 0.2. Thus they are not included in Table 2.

4.1 Triangular array

In this section we analyze in more detail the results obtained for the triangular configurations, presenting in Figure 5 the cases that show the lowest and the highest misfit values for each determined number of geophones. The dispersion curves, including the standard deviation ranges, are represented together with the theoretical array responses and the theoretical k limits.

By removing one geophone from the original triangular layout, the theoretical array response obtained for all the tested geometries maintain the central symmetry and

the differences experimented in the dispersion curves are insignificant, being 'T.6.5' and 'T.6.1' the best and worst combinations, respectively (A.T.1, Figure 5a).

When two or more stations are removed, then more attention has to be paid to the central symmetry of the theoretical response, as some of the modified arrays might highlight a particular direction or azimuth.

In case of removing two geophones, the dispersion curves obtained for all the tested modified arrays are included inside the mean value ± standard deviation range of the dispersion curve obtained for the original array, presenting then very slight differences among them. In this case, 'T.5.4' and 'T.5.7' provide the best and worst combinations, respectively (A.T.2, Figure 5b).

When three or four geophones are removed, the standard deviation of the dispersion curves obtained for the modified arrays is higher than the one obtained for the original array, even though some of the analyzed cases present very low misfit values.

For the three geophones removal, the good or acceptable geometries, according to their misfit values, are the ones with a theoretical array response showing a clear central symmetry (e.g. 'T.4.2' with m=0.0661, in Figure 6a and A.T.3). In contrast, the unacceptable geometries use to present a theoretical array response that highlights some particular direction (e.g. 'T.4.5' which is the worst analyzed case, in Figure 5c and A.T.3). At this point, it is important to comment the particular situation provided by the best geometry (i.e., 'T.4.11' in Figure 5c and A.T.4). In this case, the theoretical array response is lined up respecting to the horizontal view, but the obtained misfit value is the minimum of all the analyzed cases. This is probably because the characteristics of the recorded ambient noise that enhance the obtained results for this array configuration. We

can test this situation when we compare it with the results obtained with the array 'T.4.9' (in Figure 6b and A.T.4). In this configuration, the theoretical array response is lined up in the vertical view (perpendicular to the one obtained by the 'T.4.11') and the misfit value is 0.5403, close to the worst analyzed configuration. Thus, even though the geometry 'T.4.11' provides the minimum misfit value, we recommend to avoid it, as its theoretical array response does not present central symmetry and then, the goodness of the obtained dispersion curve might depend on the direction of the incoming ambient noise.

When four geophones are removed, some layouts also provide good dispersion curves like 'T.3.5' or 'T.3.7', despite most of them are only acceptable like 'T.3.2' or 'T.3.9' or unacceptable, e.g. 'T.3.1' or 'T.3.3' (see A.T.4 and A.T.5). The 3-stations layouts forming equilateral triangles with the shortest inter-station distances are the ones that generally provide the best dispersion curves. Figure 5d displays 'T.3.7' as the best configuration, with central symmetry in the theoretical response. In the other hand, 'T.3.10', which is a linear configuration, shows the worst result.

4.2 Circular array

Secondly, we comment the results obtained for the circular geometry, which is, in fact, an 8-stations array, as stated before. In Figure 7 we present the dispersion curves of the cases that show the lowest and the highest misfit values for each number of geophones, including the standard deviation ranges. The theoretical responses and the k limits are also displayed.

When one, two or three stations are removed, we can observe that the good or acceptable dispersion curves, according to their misfit values, are the ones with theoretical array responses showing a clear central symmetry (e.g. 'C.7.3', 'C.6.6' or 'C.5.13' which are the best analyzed cases, in Figure 7a-c and A.C.1 to A.C.5). In contrast, the analyzed unacceptable geometries present theoretical array responses that highlight some particular direction (e.g. 'C.7.6', 'C.6.11' or 'C.5.4' which are the worst analyzed cases, in Figure 7a-c and A.C.1 to A.C.5).

In the case of one station removal, the worst analyzed geometry provides also a good dispersion curve that matches very well to the one obtained through the original array. Nevertheless, as it was commented previously for the triangular configurations, we recommend avoiding any geometry without central symmetry in the theoretical array response.

When four or five stations are removed, then it is difficult to find geometries that provide central symmetry in the theoretical array response. In these cases, most of the obtained dispersion curves are acceptable or unacceptable, according to their misfit value, with a standard deviation higher than the one obtained for the original array. In Figure 7d and 7e, the best and the worst analyzed geometries are shown.

In the case of three aligned geophones ('C.3.10' in Figure 7e), the obtained dispersion curve presents some abrupt changes that may be due to instabilities in the computation process, since such dispersion curve does not correspond to any realistic physic structure of the ground.

4.3 Polygonal array

For the polygonal geometry, the dispersion curves of the cases that show the lowest and the highest misfit values for each number of geophones, including the standard deviation ranges, are represented in Figure 8. We also include the theoretical array responses and the k limits for each layout.

The original polygonal layout does not present a clear central symmetry in the theoretical array response (Figure 1c), what means a higher sensibility to the lack of some stations.

When only one geophone is removed from the analyzed layouts (Figure 8a), the central symmetry of the theoretical array responses is almost maintained, and the obtained dispersion curves fit well to the one obtained through the original array.

The suppression of more stations evidences the sensibility of the theoretical array response in the polygonal geometry, as some particular direction might be clearly highlighted, even by removing only two geophones. This is shown for 7 and 6-stations layouts in Figures 8b and 8c. Despite of providing good or acceptable dispersion curves in any case, the central symmetry of the theoretical array responses is not clear. The best cases, 'P.7.1' and 'P.6.1', highlight the vertical view, while the worst ones enhance an oblique direction. Thus, directionality in the incoming noise is going to be more determinant in the quality of the calculated dispersion curves than in previous geometries.

By removing four, five or six geophones, the possibility of obtaining more regular geometries increases. Layouts with central symmetry in the theoretical array response coincide with the best estimated dispersion curves, as it is shown in Figures 8d, 8e and 8f. On the other hand, aligned or sparse geometries, which provide theoretical array

responses lined up in some preferential directions, are generally related to the worst dispersion curves.

For 5-stations layouts, good dispersion curves are presented from layouts ‘P.5.1’ to ‘P.5.12’ and acceptable ones from ‘P.5.13’ to ‘P.5.14’ (see A.P.5 to A.P.7), according to the misfit values. When five geophones are removed (i.e., 4-stations layouts), from ‘P.4.1’ to ‘P.4.7’ the dispersion curves are good, while from layouts ‘P.4.8’ to ‘P.4.10’ they are only acceptable (see A.P.7 to A.P.9). With six geophones less, there are no good dispersion curves and only for layout ‘P.3.1’ the dispersion curve can be considered as acceptable.

4.4 Common inferences of the array optimization study

Evaluating the statistical information presented in Table 2, we can state that among the 6-stations arrays, the triangular combination clearly provides the best results, with misfit values always below 0.2. The other two layouts show higher error values, though most of the curves can be considered as good ones anyway.

For the 5-stations combinations, the triangular geometry also provides the most stable dispersion curves, with more than 90% of the cases showing misfit values down 0.2. Between the circular and the polygonal array, second one presents clearly better results with more good and less unacceptable dispersion curves.

When four geophones are considered, the triangular combinations generally show the best results, but very close to the polygonal ones. Indeed, the polygonal geometry provides more cases of good curves than the triangular one. The difference lies in the percentage of acceptable curves, which for the triangular layout is double than for the

polygonal one. Meanwhile, the circular configuration shows more than a 50% of unacceptable curves.

Finally, for the 3-stations layouts, the triangular array is the only geometry that shows good dispersion curves with a 20% of the cases with misfit values below 0.2. The configurations that generally provide the best results correspond to equilateral triangles with the shortest inter-station distance.

Therefore, from the study carried out, we can observe how the inclusion of fewer stations in the array design does not necessary mean a worsening in the obtained dispersion curve, when they are suitable placed. Some examples of this are 'T.3.7' front 'T.5.7' and 'T.6.1' (Figure 5, A.T.5, A.T.2 and A.T.1); 'C.3.9' front 'C.5.4' and 'C.6.11' (Figure 7, A.C.8, A.C.4 and A.C.3) or 'P.3.1' front 'P.5.16' and 'P.6.16' (Figure 8, A.P.9, A.P.7 and A.P.5).

Also for the different analyzed cases, we find that when only a reduced number of stations are available, i.e. five or less, then it is preferred to keep the proximity between the sensors in a reduced layout, despite shortening the maximum aperture of the array, e.g. 'T.3.7' (A.T.5), 'C.5.7' (A.C.4) or 'P.4.1' (A.P.7). We should avoid linear configurations, e.g. 'T.3.8' (A.T.5), 'C.4.12' (A.C.7) or 'P.4.15' (A.P.9); isolated geophones or sparse geometries, e.g. 'T.3.3' (A.T.5), 'C.4.7' (A.C.6) or 'P.4.11' (A.P.9), which might lead to theoretical array responses without central symmetry and non-reliable dispersion curves.

Respecting to the theoretical resolution limits, we can see in Figure 4 how they change as the number of geophones is reduced. The minimum resolution limit is obtained for the original layout, although it can be also reached by some modified configurations.

Thus, from the study carried out, we can conclude that the resolution limit obtained for the original layout can be used for most of the good and acceptable reduced configurations without losing the reliability of the obtained dispersion curves.

All these results have been obtained for a nearly isotropic noise wavefield (Figure 2). Therefore, the extracted inferences might be considered general only for the frequency range where the distribution of the noise sources was homogeneous in space.

4.5 Additional tests

In order to evaluate the obtained common inferences, the same kind of analysis has been repeated for other circular arrays with different apertures and different kind of instruments. These noise measurements were recorded at different sites of the Bajo Segura Basin (southeast Spain). Concretely in Almoradí (two circular arrays with 25 m and 100 m of aperture) and in Catral (circular array with 60 m of aperture). Each array was composed of nine 1Hz Mark L-4C-3D seismometers: one of them in the center of the circular layout and the other 8 distributed approximately around it. During the data acquisition, one of the perimeter stations failed, producing a similar situation to the one analyzed previously with the geophones and the circular array. More details about this field campaign can be found in Rosa-Cintas et al. (2011).

From the analysis carried out in the 25m-aperture array, we can extract the same general inferences stated in section 4.4. In Figure 9 we show the dispersion curves of the cases that show the lowest and the highest misfit values for each number of stations, together with the theoretical responses and the k limits. For this configuration, we can

check that even with only five stations it is possible to obtain geometries with central symmetry in the theoretical array responses and good or acceptable dispersion curves.

For the other analyzed arrays, with apertures of 60 m and 100 m, respectively, the obtained results are worse than the ones obtained for the previous small arrays. As the distances among the stations are higher, the lack of some of these stations affects much more to the final results. From the analysis carried out, we can conclude that at least 6 or 7-stations configurations are needed to obtain good or acceptable dispersion curves with these apertures.

Therefore, the array optimization study works better for small aperture arrays, where the reduction of some geophones does not imply a severe separation among the rest of them. In contrast, as the array aperture increases, the reduction of geophones could conduct to a small set of geophones separated by a great distance, which would result in isolated geophones or sparse geometries and then in unacceptable dispersion curves.

5. CONCLUSIONS

In this paper we have developed an experimental work to examine which is the minimum number of stations that would provide reliable dispersion curves for three prearranged array configurations: 7-geophones triangular, 9-geophones circular with central station and 9-geophones polygonal geometries.

Each one of the studied layouts is derived from a general array of 25 m of aperture, by removing a certain number of geophones before the data analysis. The circular layout provides the wider frequency range for the dispersion curve analysis, with the lowest maximum resolution limit and one of the highest aliasing limits. Whereas, the

analyzed polygonal array, conceived to join the largest aperture of the circular geometry with the shortest inter-station distances presented in the general layout, does not show very promising results. In this case, it is clear that more stations would be needed to reach the same theoretical kmin limit than for the circular configuration. Regarding the triangular layout, it presents even lower maximum resolution limit than the polygonal array, with smaller aperture, and clearly lower aliasing limit than the two 9-stations arrays.

By checking the dispersion curves obtained through the original layouts, we can notice that the three ones are very similar. The principal variation of using different array configurations is the valid frequency interval associated to each dispersion curve. In this sense, the circular and triangular geometries would be clearly preferred to the equivalent polygonal layouts.

For the array optimization study we evaluate the theoretical array responses and the differences between the dispersion curves obtained through the original and the modified arrays, by means of a misfit function. Then we use this misfit value to classify the curves as: good, acceptable or unacceptable.

The nature and direction of the incoming noise can be crucial in the final results. So we recommend designing layouts that present central symmetry in their theoretical array responses, as it was already addressed in the deliverables and guidelines of the SESAME project (i.e., SESAME, 2005).

Although this first evaluation provides insights of the good performance of the modified arrays and their theoretical wavenumber limits, it is not enough to determine the minimum number of stations that might be used without losing the capability of the

original arrays. Thus, a subsequent evaluation of the dispersion curves is required, which provides estimation about the real effects on them.

Among the tested layouts, the triangular geometry is generally less constrained by stations removing and therefore, it provides better results than the circular and the polygonal configurations. For the analyzed triangular geometries, we obtain good dispersion curves even with only three stations, whenever that the central symmetry of the theoretical array response is maintained. In this case, the best results are obtained by forming an equilateral triangle with the shortest inter-station distance.

In the case of the circular layouts, we can obtain geometries with central symmetry in the theoretical array responses and good or acceptable dispersion curves, even with only five stations. When more than four stations are removed, then it is difficult to find geometries that provide central symmetry in the theoretical array response, because with few geophones placed in the perimeter of the circle, the resulting combinations are generally aligned or sparse. Thus, most of the obtained dispersion curves are acceptable or unacceptable, with higher standard deviation than the one obtained for the original array.

Finally, the polygonal layout does not present a clear central symmetry in the original theoretical array response. This involves higher sensibility to the stations suppression, which could highlight some particular directions. As the number of geophones is reduced, more regular geometries can be obtained with clearer central symmetry in the theoretical array response. In these cases, the analyzed layouts present mostly good or acceptable dispersion curves, even with only four stations configurations.

As general conclusion, when the number of usable stations is reduced, we should try to preserve the central symmetry of the theoretical array response and to position the sensors maintaining the spatial continuity among them. From the analysis carried out in this work, we have shown that with a small-aperture, but well-configured array, it is possible to extend by far their capability of analysis in the lower frequency range, providing dispersion curves very similar to those obtained with bigger and denser (i.e., with more stations) layouts. On the other hand, by separating too much the stations, the analysis can provide bad dispersion curves at all.

The conclusions extracted from the array optimization study can be better extrapolated for small aperture arrays, where the reduction of some geophones does not imply a severe separation among the rest of them. In contrast, for large-aperture arrays, the reduction of some stations could conduct to a small set of geophones separated by a great distance, which would result in unacceptable dispersion curves. In this case, the possible reduction of the number of stations would be lower than the obtained for the small-aperture arrays.

Obviously, attending to the present study, if we had nine stations or more, we would use all of them for the field campaign. However this is not the real situation for many small research groups, where the number of available stations is very limited by the economic support. In these circumstances, the developed study acquires a significant usefulness, providing some guidelines to maximize the analysis capability of the arranged arrays when using a reduced number of stations.

6. ACKNOWLEDGEMENTS

This work has been developed thanks to the financial support of the Spanish Government (CGL2011-30153-C02-02/BTE and CGL2011-25162), Programa de FPU del Ministerio de Ciencia e Innovación (AP2008-04686) and Instituto Alicantino de Cultura Juan Gil-Albert. We are very grateful also to the Local Seismic Network of the University of Alicante (supported by Diputación de Alicante) that provided us the geophones and especially to Dr. P. Jáuregui for his help with the instrumentation. Finally, we want to thank the anonymous reviewers for their comments and suggestions to improve the quality of this paper, as well as to the Journal Manager, Chandini Emmanuel, and the editor-in-chief, Klaus Holliger, for their contribution to the final result.

7. REFERENCES

Aki, K., 1957. Space and time spectra of stationary stochastic waves, with special reference to microtremors. Bulletin of the Earthquake Research Institute 35, 415–456.

Alfaro, P., Andreu, J.M., Delgado, J., Estévez, A., Soria, J.M., Teixidó, T., 2002. Quaternary deformation of the Bajo Segura blind fault (eastern Betic Cordillera, Spain) revealed by high-resolution reflection profiling. Geological Magazine 139, 331–341.

Asten, M.W., Henstridge, J.D., 1984. Array estimators and the use of microseisms for reconnaissance of sedimentary basins. Geophysics 49, 1828–1837.

Asten, M.W., Lam, N., Gibson, G., Wilson, J., 2000. Microtremor survey design optimised for application to site amplification and resonance modelling, in: Griffith, M., Love, D., McBean, P., McDougall, A., Butler, B. (Eds.), Total Risk Management

in the Privatised Era. Proceedings of Conference, Australian Earthquake Engineering Soc., Adelaide, paper 7.

Asten, M.W., Dhu, T., Lam, N., 2004. Optimised array design for microtremor array studies applied to site classification; comparison of results with SCPT Logs, in: Proceedings of the 13th World Conference on Earthquake Engineering, Vancouver, paper 2903.

Asten, M.W., 2006. On bias and noise in passive seismic data from finite circular array data processed using SPAC methods. Geophysics 71, 153–162.

Barber, N.S., 1959. Design of 'optimum' arrays for direction finding. Electronic and Radio Engineering 36, 222–232.

Bard, P.-Y., 1994. Effects of surface geology on ground motion: recent results and remaining issues, in: Proceedings of the 10th European Conference on Earthquake Engineering, Vienna, pp. 305–323.

Boxberger, T., Picozzi, M., Parolai, S., 2011. Shallow geology characterization using Rayleigh and Love wave dispersion curves derived from seismic noise array measurements. Journal of Applied Geophysics 75, 345–354.

Capon, J., 1969. High-resolution frequency-wavenumber specrum analysis, in: Proceedings of the IEEE 57, 1408–1418.

Chávez-García, F., Rodríguez, M., Stephenson, W., 2005. An alternative approach to the SPAC analysis of microtremors: Exploiting stationarity of noise. Bulletin of the Seismological Society of America 95, 277–293.

Cho, I., Tada, T., Shinozaki, Y., 2004. A new method to determine phase velocities of Rayleigh waves from microseisms. Geophysics 69, 1535–1551.

Cho, I., Tada, T., Shinozaki, Y., 2006. Centerless circular array method: Inferring phase velocities of Rayleigh waves in broad wavelength ranges using microtremor records. Journal of Geophysical Research 111, B09315, doi: 10.1029/2005JB004235.

Cho, I., Tada, T., Shinozaki, Y., 2008. Assessing the applicability of the spatial autocorrelation method: A theoretical approach. Journal of Geophysical Research 113, B06307, doi: 10.1029/2007JB005245.

Chouet, B., De Luca, G., Milana, G., Dawson, P., Martini, M., Scarpa, R., 1998. Shallow velocity structure of Stromboli Volcano, Italy, derived from small aperture array measurements of Strombolian tremor. Bulletin of the Seismological Society of America 88, 653–666.

Chun-Hsiang, K., Ding-Shing, C., Hung-Hao, H., Tao-Ming, C., Hsien-Jen, C., Che-Min, L., Kuo-Liang, W., 2009. Comparison of three different methods in investigating shallow shear-wave velocity structures in Ilan, Taiwan. Soil Dynamics and Earthquake Engineering 29, 133–143.

Claprood, M., Asten, M.W., 2010. Statistical Validity Control on SPAC Microtremor Observations Recorded with a Restricted Number of Sensors. Bulletin of the Seismological Society of America 100 (2), 776–791.

D'Amico, V., Picozzi, M., Baliva, F., Albarello, D., 2008. Ambient Noise Measurements for Preliminary Site-Effects Characterization in the Urban Area of Florence, Italy. Bulletin of the Seismological Society of America 98, 1373–1388.

Delgado, J., López Casado, C., Estévez, A., Giner, J., Cuenca, A., Molina, S., 2000. Mapping soft soils in the Segura river valley (SE Spain): a case study of microtremors as an exploration tool. Journal of Applied Geophysics 45, 19–32.

Delgado, J., Alfaro, P., Andreu, J.M., Cuenca, A., Doménech, C., Estévez, A., Soria, J.M., Tomás, R., Yébenes, A., 2003. Engineering-geological model of the Segura River flood plain (SE Spain): a case study for engineering planning. Engineering Geology 68, 171–187.

Endrun, B., Ohrnberger, M., Savvaidis, A., 2010. On the repeatability and consistency of three-component ambient vibration array measurements. Bulletin of Earthquake Engineering 8, 535–570.

Galiana-Merino, J.J., Mahajan, A.K., Lindholm, C., Rosa-Herranz, J., Mundepi, A.K., Rai, N., 2011. Seismic noise array measurements using broadband stations and vertical geophones: preliminary outcomes for the suitability on f-k analysis. Bulletin of Earthquake Engineering 9, 1309–1325.

Haubrich, R.A., 1968. Array design. Bulletin of the Seismological Society of America 58, 977–991.

Horike, M., 1985. Inversion of phase velocity of long-period microtremors to the S-wave-velocity structure down to the basements in urbanized areas. Journal of Physics of the Earth 33, 59–96.

Kind, F., Fäh, D., Giardini, D., 2005. Array measurements of S-wave velocities from ambient vibrations. Geophysical Journal International 160, 114–126.

Lacoss, R.T., Kelly, E.J., Toksöz, M.N., 1969. Estimation of seismic noise structure using arrays. Geophysics 34, 21–38.

Lebrun, B., Hatzfeld, D., Bard, P.-Y., 2001. A site effect study in urban area: experimental results in Grenoble (France). Pure and Applied Geophysics 158, 2543–2557.

Mahajan, A.K., Galiana-Merino, J.J., Lindholm, C., Arora, B.R., Mundepi, A.K., Rai, N., Chauhan, N., 2011. Characterization of the sedimentary cover at the Himalayan foothills using active and passive seismic techniques. Journal of Applied Geophysics 73, 196–206.

Martínez Solares, J.M., Mézcua, J., 2002. *Catálogo Sísmico de la Península Ibérica (880 a.c. - 1900)*. Monografía Núm. 18.

Mundepi, A.K., Galiana-Merino, J.J., Kamal, Lindholm, C., 2010. Soil characteristics and site effect assessment in the city of Delhi (India) using H/V and f-k methods. Soil Dynamics and Earthquake Engineering 30, 591–599.

Nakamura, Y. (1989). A method for dynamic characteristics estimation of subsurface using microtremors on the ground surface, Quarterly Report of the Railway Technical Research Institute Japan 30, 25–33.

Ohori, M., Nobata, A., Wakamatsu, K., 2002. A comparison of ESAC and FK methods of estimating phase velocity using arbitrarily shaped microtremor analysis. Bulletin of the Seismological Society of America 92, 2323–2332.

Ohrnberger, M., 2001. Continuous automatic classification of seismic signals of volcanic origin at Mt Merapi, Java, Indonesia. Dissertation, University of Potsdam.

Ohrnberger, M., Scherbaum, F., Krüger, F., Pelzing, R., Reamer, S.K., 2004. How good are shear-wave velocity models obtained from inversion of ambient vibrations in the lower Rhine embayment (N.W. Germany)? Bollettino di Geofisica Teorica ed Applicata 45, 215–232.

Okada, H., 2003. The Microtremor Survey Method, Geophysical Monograph series 12, M. W. Asten (Editor), Society of Exploration Geophysicist, Tulsa, Oklahoma.

Okada, H., 2006. Theory of efficient array observations of microtremors with special reference to the SPAC method. Exploration Geophysics 37, 73–85.

Parolai, S., Richwalski, S.M., Milkereit, C., Fäh, D., 2006. S-wave velocity profiles for earthquake engineering purposes for the Cologne area (Germany), Bulletin of Earthquake Engineering 4, 65–94.

Parolai, S., Mucciarelli, M., Gallipoli, M.R., Richwalski, S.M., Strollo, A., 2007. Comparison of Empirical and Numerical Site Responses at the Tito Test Site, Southern Italy. Bulletin of the Seismological Society of America 97, 1413–1431.

Parolai, S., Orunbaev, S., Bindi, D., Strollo, A., Usupaev, S., Picozzi, M., Di Giacomo, D., Augliera, P., D'Alema, E., Milkereit, C., Moldobekov, B., Zschau, J., 2010. Site Effects Assessment in Bishkek (Kyrgyzstan) Using Earthquake and Noise Recording Data. Bulletin of the Seismological Society of America 6, 3068–3082.

Picozzi, M., Strollo, A., Parolai, S., Durukal, E., Özel, O., Karabulut, S., Zschau, J., Erdik, M., 2009. Site characterization by seismic noise in Istanbul, Turkey. Soil Dynamics and Earthquake Engineering 29, 469–482.

Picozzi, M., Parolai, S., Bindi, D., 2010. Deblurring of frequency-wavenumber images from small-scale seismic arrays. Geophysical Journal International 181, 357–368.

Poggi, V., Fäh, D., 2010. Estimating Rayleigh wave particle motion from three-component array analysis of ambient vibrations. Geophysical Journal International 180, 251–267.

Roberts, J.C., Asten, M.W., 2004. Resolving a velocity inversion at the geotechnical scale using the microtremor (passive seismic) survey method. Exploration Geophysics 35, 14–18.

Rosa-Cintas, S., Galiana-Merino, J.J., Molina-Palacios, S., Rosa-Herranz, J., García-Fernández, M., Jiménez, M.J., 2011. Soil characterization in urban areas of the Bajo Segura Basin (Southeast Spain) using H/V, F–K and ESAC methods. Journal of Applied Geophysics 75, 543–557.

Rosa-Cintas, S., Galiana-Merino, J.J., Rosa-Herranz, J., Molina, S., Martínez-Esplá, J.J., 2012a. Polarization analysis in the stationary wavelet packet domain: Application to HVSR method. Soil Dynamics and Earthquake Engineering 42, 246–254.

Rosa-Cintas, S., Galiana-Merino, J.J., Rosa-Herranz, J., Molina, S., Giner-Caturla, J., 2012b. Suitability of 10 Hz vertical geophones for seismic noise array measurements based on frequency-wavenumber and extended spatial autocorrelation analyses. Geophysical Prospecting, doi: 10.1111/j.1365-2478.2012.01114.x.

SESAME, Site Effects Assessment Using Ambient Excitations, 2005. WP13, Recommendations for quality array measurements and processing. Deliverable D24.13. European Commission – Research General Directorate. Project No. EVG1-CT-2000-00026.

Soria, J., Alfaro, P., Estévez, A., Delgado, J., Durán, J.J., 1999. The Holocene sedimentation rates in the Lower Segura Basin (eastern Betic Cordillera, Spain): eustatic implications. Bulletin de la Societe Geologique de France 170, 349–354.

Souriau, A., Roullé, A., Ponsolles, C., 2007. Site Effects in the City of Lourdes, France, from H/V Measurements: Implications for Seismic-Risk Evaluation. Bulletin of the Seismological Society of America 97, 2118–2136.

Stephenson, W.J., Hartzell, S., Frankel, A.D., Asten, M., Carver, D.L., Kim, W.Y., 2009. Site characterization for urban seismic hazards in lower Manhattan, New York City,

from microtremor array analysis. Geophysical Research Letters, 36, L03301, doi: 10.1029/2008GL036444.

Strollo, A., Parolai, S., Jäckel, K.-H., Marzorati, S., Bindi, D., 2008a. Suitability of short-period sensors for retrieving reliable H/V peaks for frequencies less than 1 Hz. Bulletin of the Seismological Society of America 98(2), 671–681.

Strollo, A., Bindi, D., Parolai, S., Jäckel, K.-H., 2008b. On the suitability of 1s geophone for ambient noise measurements in the 0.1-20 Hz frequency range: experimental outcomes. Bulletin of Earthquake Engineering 6, 141–147.

Wathelet, M., 2005. *Array recordings of ambient vibrations: surface-wave inversion*. PhD thesis, Université de Liège (Belgium).

Toksöz, M.N. and Lacoss R. T. (1968). Microseisms: Mode Structure and Sources. *Science*. Vol. 159, pp. 872-873.

TABLES

Table 1: Wavenumber limits (in rad/m) for the three original array geometries.

Array Geometry	kmin/2	kmax
Circular	0.096	1.065
Triangular	0.127	0.604
Polygonal	0.164	1.073

Table 2: Different analyzed cases grouped according to the number of geophones and the obtained misfit values. In the first column we specify in brackets the number of cases done for each layout. In the other columns we put into brackets the number of cases that accomplish the misfit criterion respect to the all tested.

Six geophones			
Misfit (m)	$m \leq 0.2$	$0.2 < m \leq 0.5$	$0.5 < m$
Triangular (5)	(5/5) **100.0%**		
Circular (15)	(14/15) **93.3%**		(1/15) **6.7%**
Polygonal (16)	(14/16) **87.5%**	(2/16) **12.5%**	

Five geophones			
Misfit (m)	$m \leq 0.2$	$0.2 < m \leq 0.5$	$0.5 < m$
Triangular (11)	(10/11) **90.9%**	(1/11) **9.1%**	
Circular (17)	(10/17) **58.8%**	(2/17) **11.8%**	(5/17) **29.4%**
Polygonal (16)	(12/16) **75.0%**	(2/16) **12.5%**	(2/16) **12.5%**

Four geophones			
Misfit (m)	$m \leq 0.2$	$0.2 < m \leq 0.5$	$0.5 < m$
Triangular (14)	(6/14) **42.9%**	(6/14) **42.9%**	(2/14) **14.3%**
Circular (14)	(2/14) **14.3%**	(4/14) **28.6%**	(8/14) **57.1%**
Polygonal (16)	(7/16) **43.7%**	(3/16) **18.8%**	(6/16) **37.5%**

Three geophones			
Misfit (m)	$m \leq 0.2$	$0.2 < m \leq 0.5$	$0.5 < m$
Triangular (10)	(2/10) **20.0%**	(4/10) **40.0%**	(4/10) **40.0%**
Circular (10)		(2/10) **20.0%**	(8/10) **80.0%**
Polygonal (16)		(1/16) **6.3%**	(15/16) **93.7%**

FIGURE CAPTIONS

Figure 1. Array configurations: (a) triangular, (b) circular with central station and (c) polygonal. The theoretical array responses are also shown in the right panels.

Figure 2. Examples of the f-k analysis for 4, 6, 8 and 10 Hz using the circular array configuration.

Figure 3. Dispersion curves calculated for the original geometries, including the wavenumber limits functions for kmax/2 and kmin/2 values. The valid frequency intervals for each dispersion curve are marked with color areas, according to the intersection of the dispersion curves and the wavenumber limits functions for kmax/2 and kmin/2 values (Wathelet, 2005).

Figure 4. Theoretical resolution limit of the original layout and theoretical resolution limit ranges (i.e. the range between the minimum and maximum kmin/2 values) of the reduced configurations that provide at least acceptable results. The resolution limits are shown for the triangular (a), circular (b) and polygonal (c) arrays.

Figure 5. Theoretical array response with the k limits (left panels) and dispersion curves (right panel) for the geometries that present the lowest (left column) and highest (right column) misfit values for different number of sensors in the triangular array: 6 (a), 5 (b), 4 (c) and 3 (d). In all the cases, the dispersion curves of the modified arrays are compared with the dispersion curve corresponding to the original triangular array, showing their mean value and their associated standard deviation.

Figure 6. a) Modified triangular array ('T.4.2') with central symmetry in the theoretical array response and with one of the lowest misfit values. b) Modified triangular array ('T.4.9') with the theoretical array response lined up in the vertical view (perpendicular to the one obtained by the 'T.4.11') and the misfit value close to the worst analyzed geometry.

Figure 7. Theoretical array response with the k limits (left panels) and dispersion curves (right panel) for the geometries that present the lowest (left column) and highest (right column) misfit values for different number of sensors in the circular array: 7 (a), 6 (b), 5 (c), 4 (d) and 3 (e). In all the cases, the dispersion curves of the modified arrays are compared with the dispersion curve corresponding to the original circular array, showing their mean value and their associated standard deviation.

Figure 8. Theoretical array response with the k limits (left panels) and dispersion curves (right panel) for the geometries that present the lowest (left column) and highest (right column) misfit values for different number of sensors in the polygonal array: 8 (a), 7 (b), 6 (c), 5 (d), 4 (e) and 3 (f). In all the cases, the dispersion curves of the modified arrays are compared with the dispersion curve corresponding to the original polygonal array, showing their mean value and their associated standard deviation.

Figure 9. Theoretical array response with the k limits (left panels) and dispersion curves (right panel) for the geometries that present the lowest (left column) and highest (right column) misfit values for different number of sensors in the 25m-aperture array of Almoradí: 7 (a), 6 (b), 5 (c), 4 (d) and 3 (e). In all the cases, the dispersion curves of the modified arrays are compared with the dispersion curve corresponding to the original circular array, showing their mean value and their associated standard deviation.

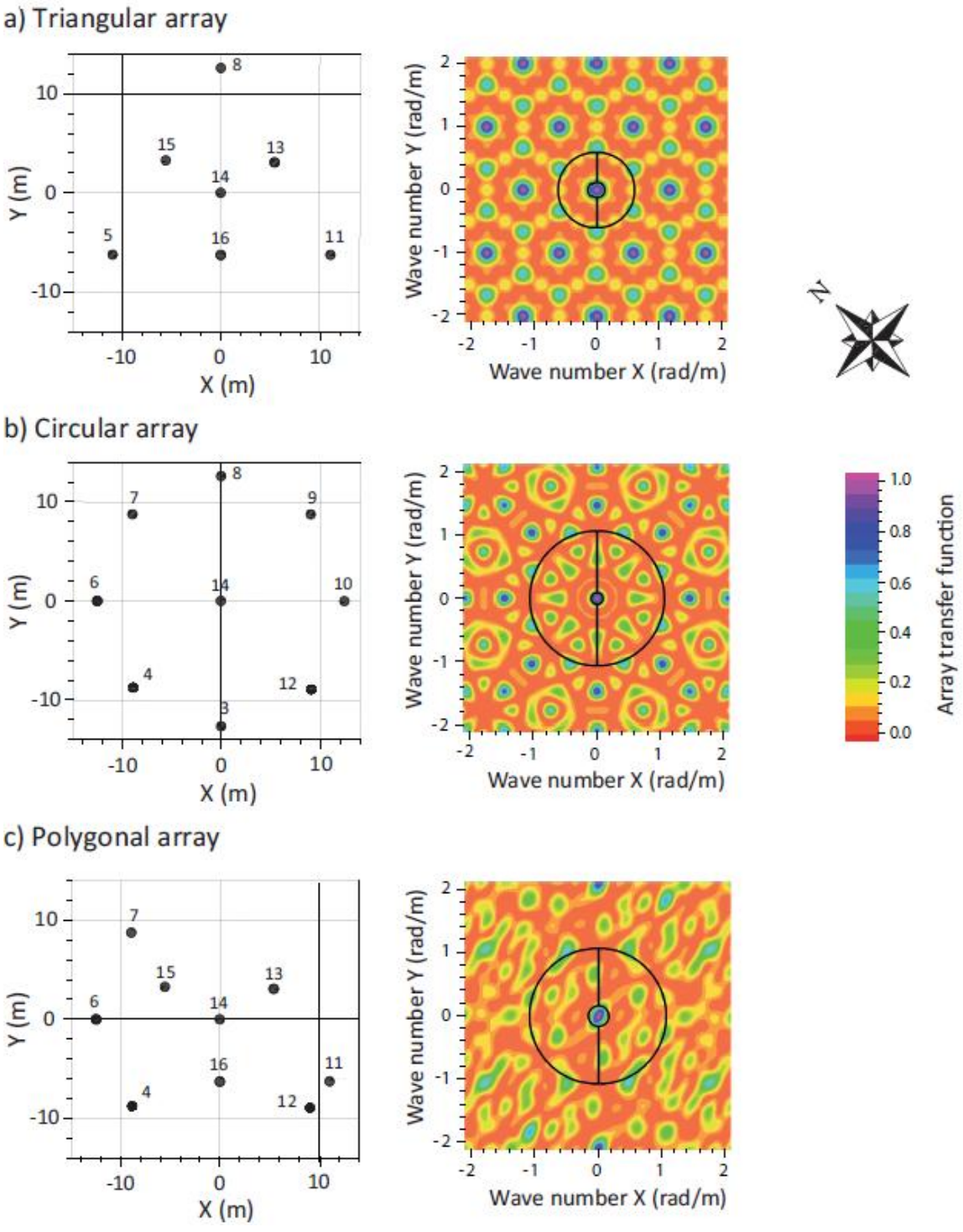
a) Triangular array
b) Circular array
c) Polygonal array
Y (m)
X (m)
Wave number Y (rad/m)
Wave number X (rad/m)
N
Array transfer function
1.0
0.8
0.6
0.4
0.2
0.0

Fig 1

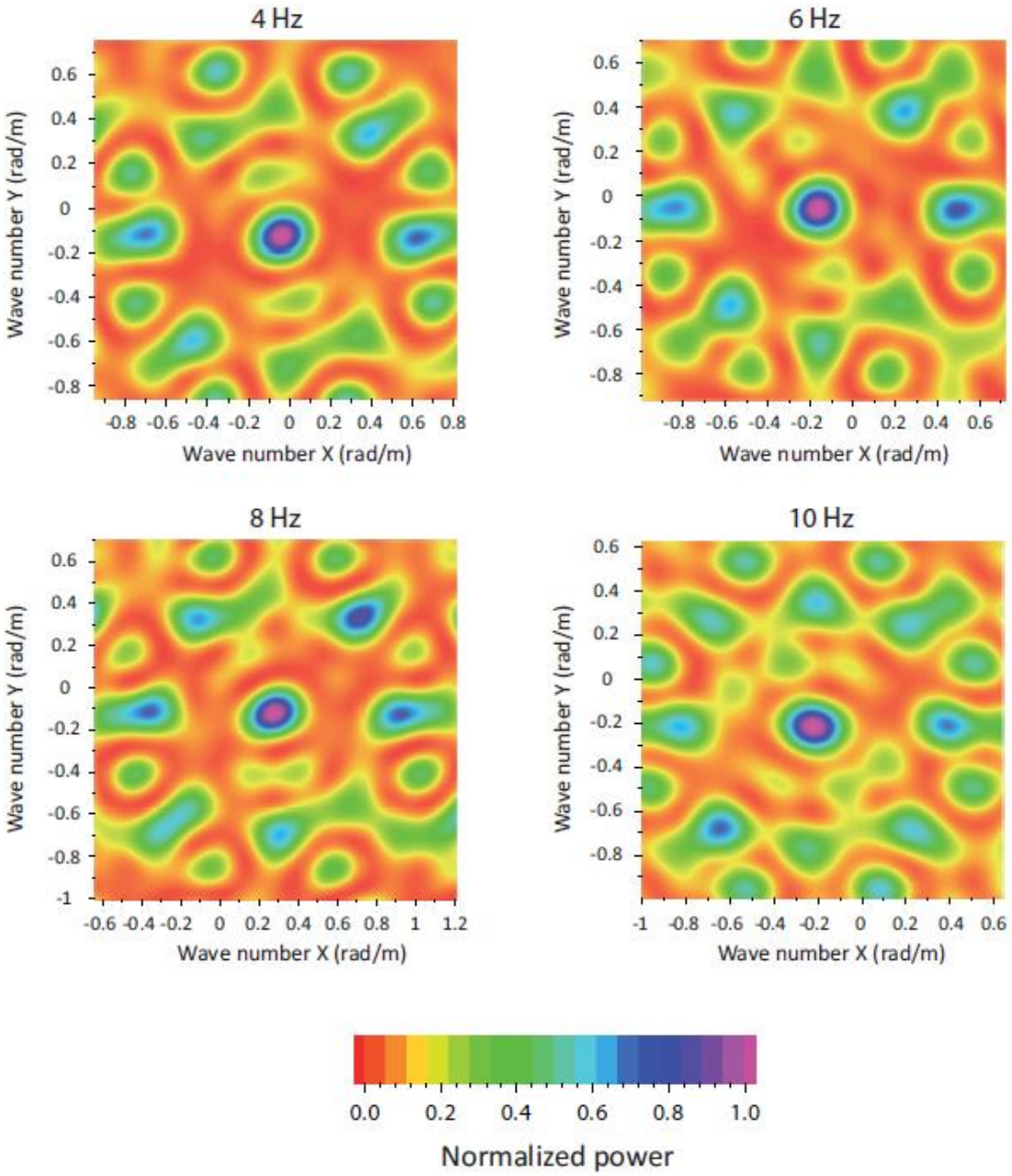

Fig 2

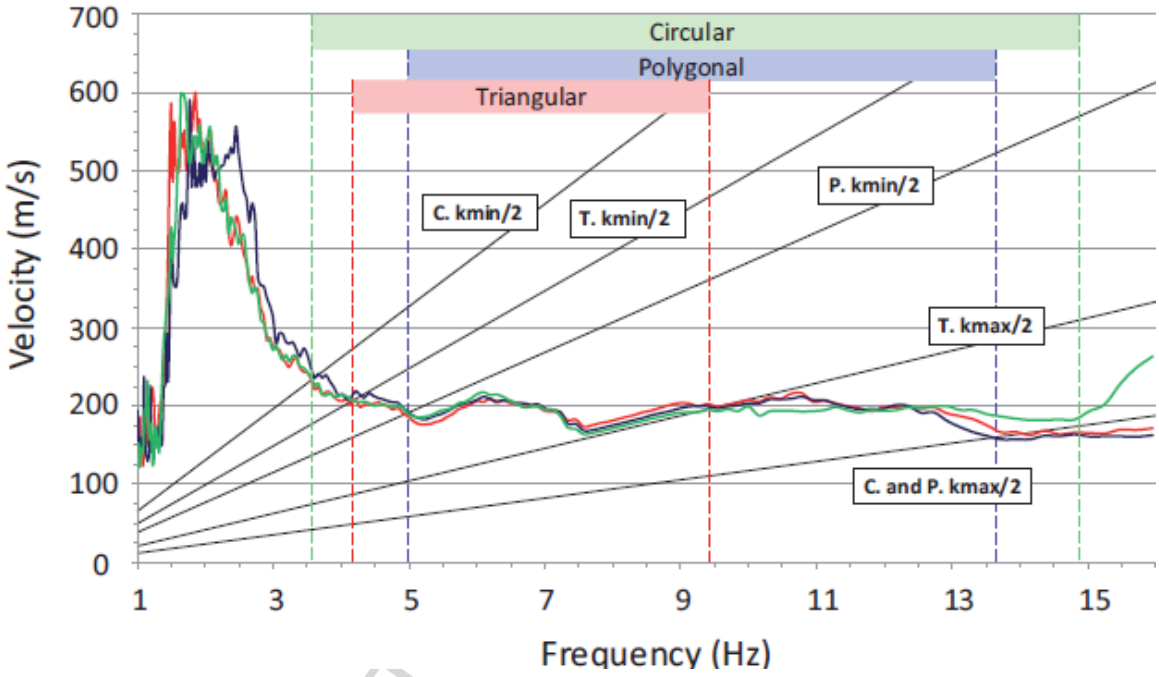

Fig 3

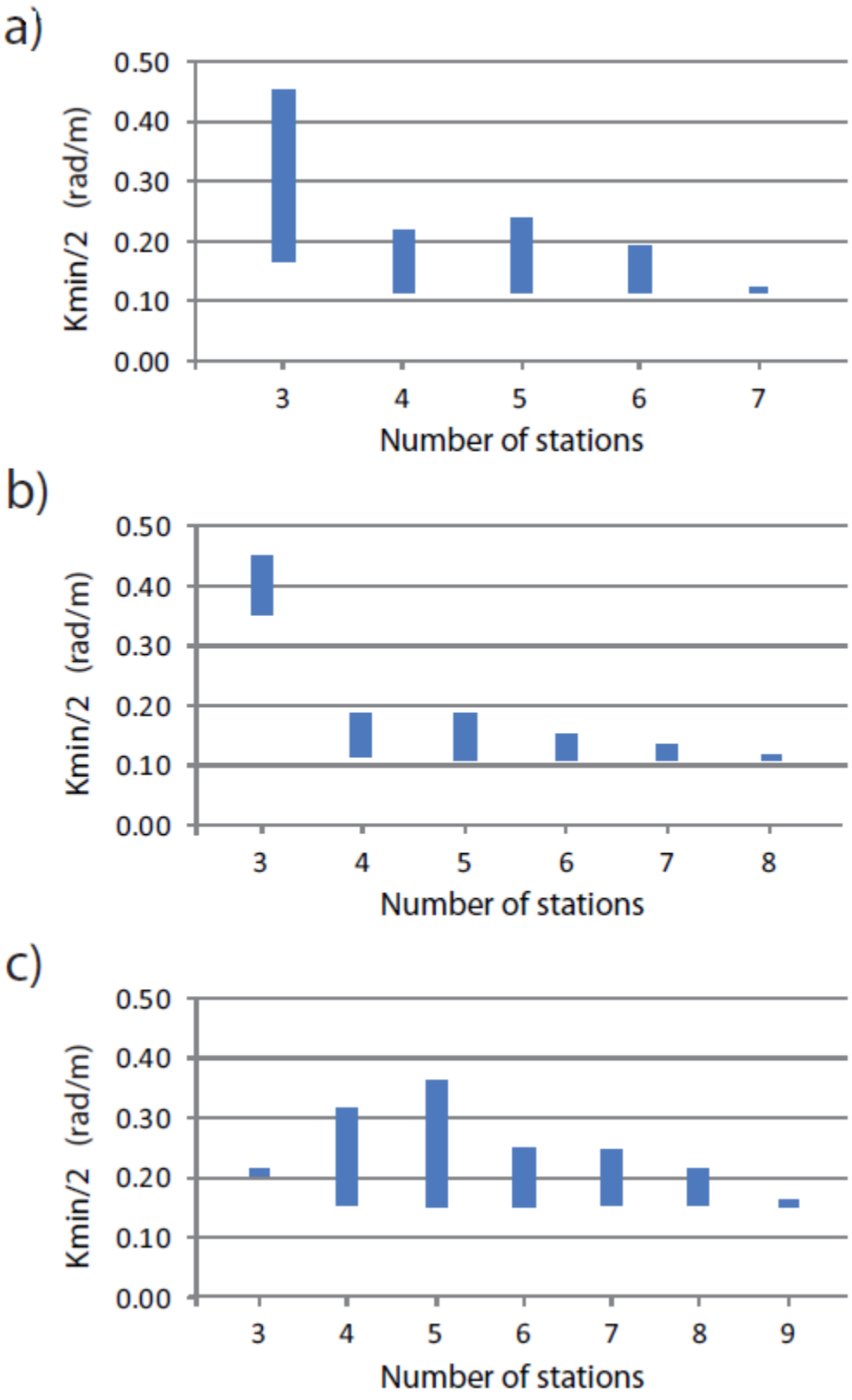

Fig 4

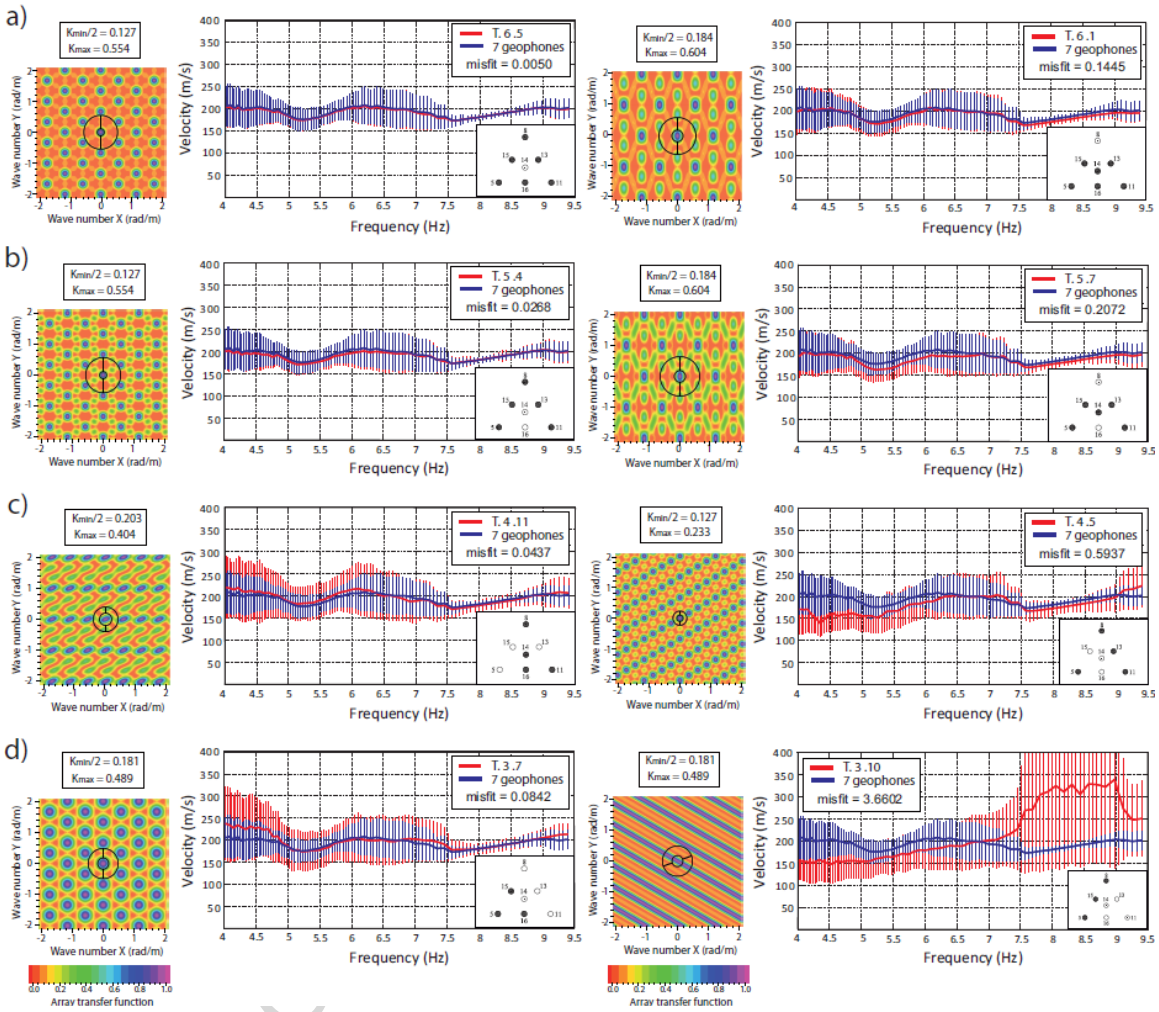

Fig 5

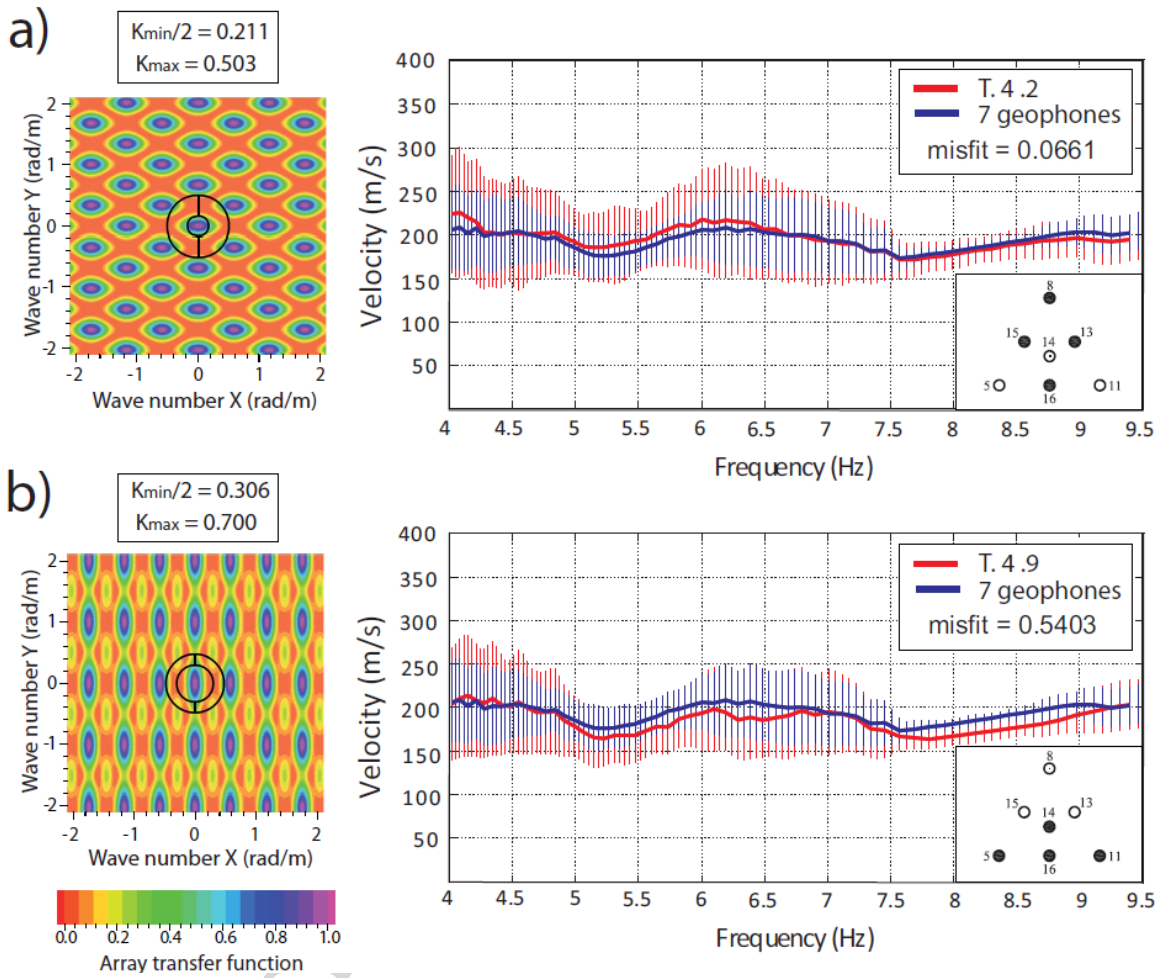

Fig 6

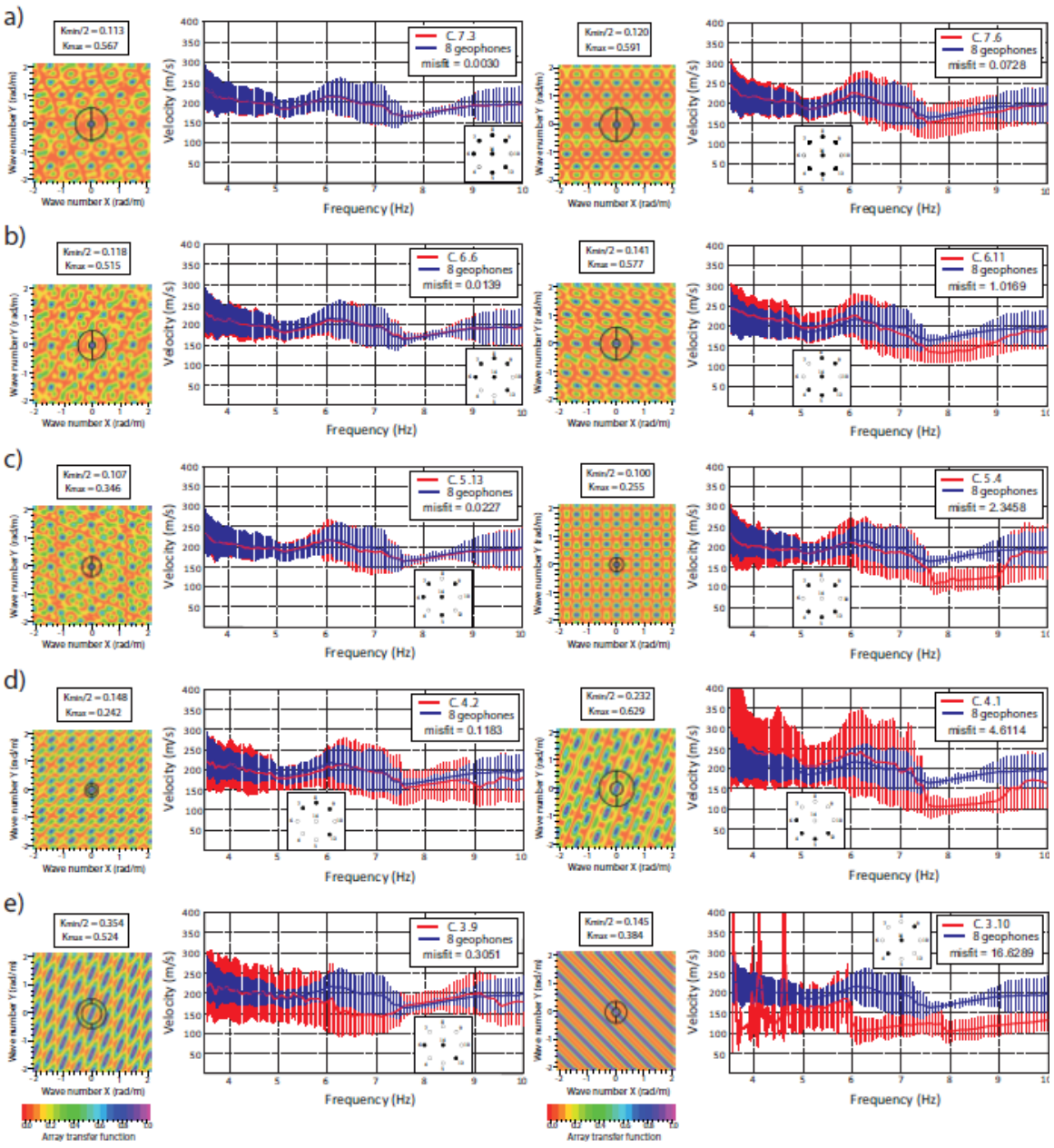

Fig 7

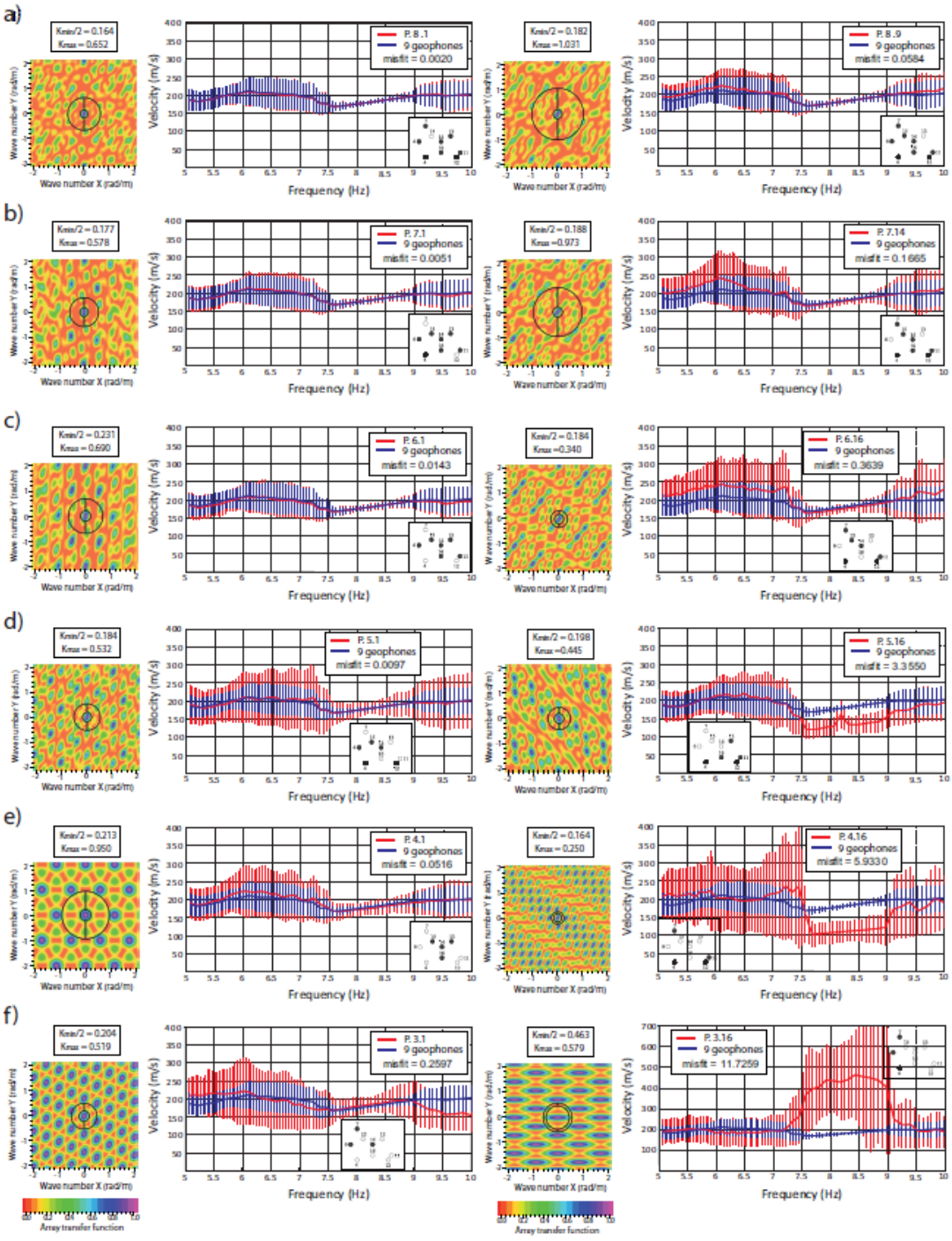

Fig 8

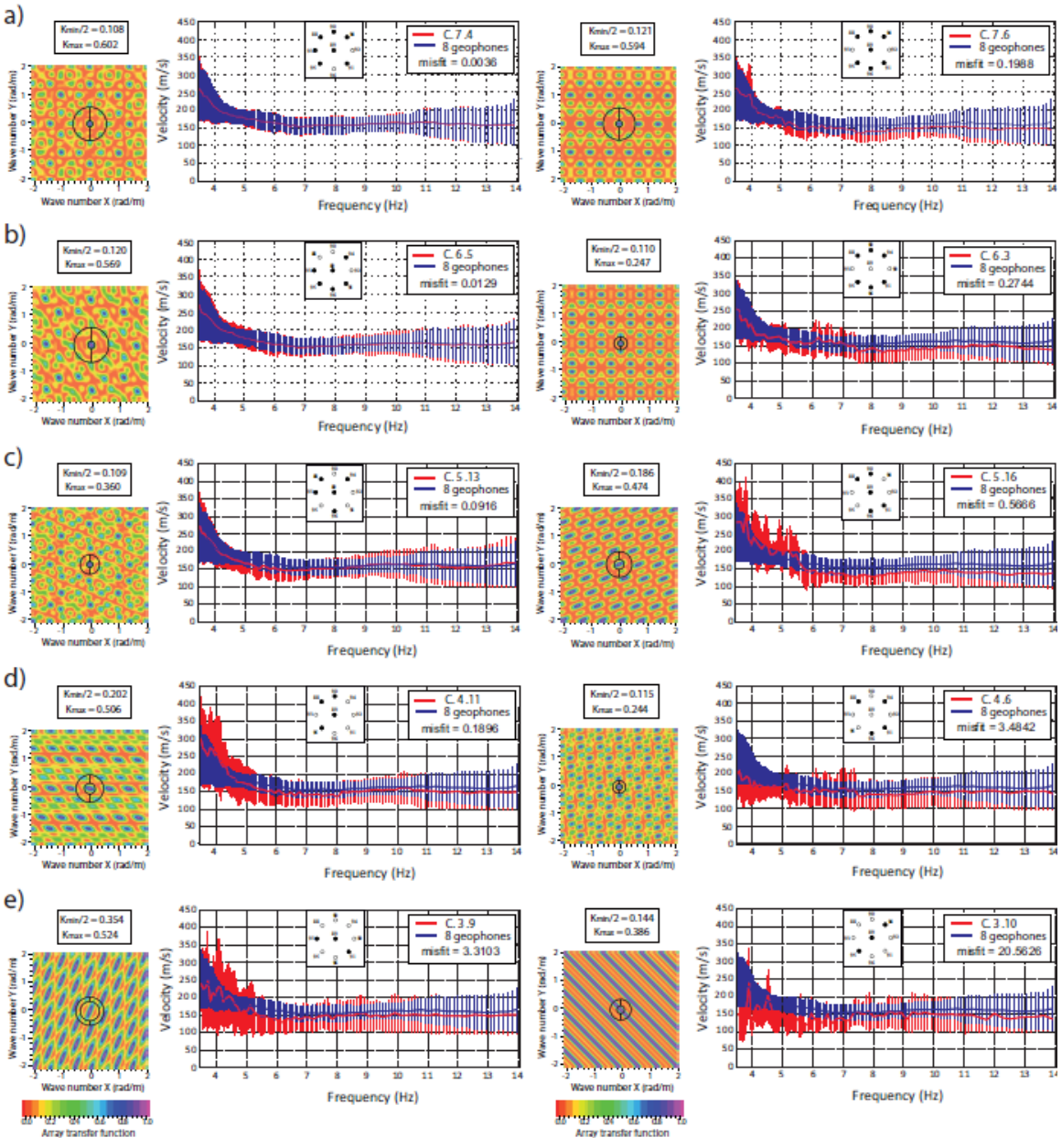

Fig 9

Highlights

- We analyze the stations suppression influence in the dispersion curve calculation.
- We compare 3 array layouts: triangular, circular with central station and polygonal.
- Comparison of the obtained dispersion curves is done by means of a misfit function.
- The study improves future array designs by optimizing the number of stations arranged.